HHS Public Access

Author manuscript

Arch Biochem Biophys. Author manuscript; available in PMC 2024 August 01.

Published in final edited form as:

Arch Biochem Biophys. 2023 August ; 744: 109702. doi:10.1016/j.abb.2023.109702.

The DUSP Domain of Pseudophosphatase MK-STYX Interacts with G3BP1 to Decrease Stress Granules

Jonathan Smailys[1], **Fei Jiang**[1], **Tatiana Prioleau**[1], **Kylan Kelley**[1,3], **Olivia Mitchell**[2], **Samah Nour**[3], **Lina Ali**[3], **William Buchser**[3], **Lynn Zavada**[1], **Shantá D. Hinton**[1,*]

[1]Department of Biology, Integrated Science Center, William and Mary, Williamsburg, VA, 23185, USA

[2]Department of Biology, Hampton University, Hampton, VA, 23666

[3]Department of Genetics, Washington University, St. Louis, MO, 63110, USA

Abstract

Mitogen activated protein kinase phosphoserine/threonine/tyrosine-binding protein (MK-STYX) is a dual specificity (DUSP) member of the protein tyrosine phosphatase family. It is a pseudophosphatase, which lacks the essential amino acids histidine and cysteine in the catalytic active signature motif (HCX_5R). We previously reported that MK-STYX interacts with G3BP1 [Ras-GAP (GTPase-activating protein) SH3 (Src homology 3) domain-binding-1] and reduces stress granules, stalled mRNA. To determine how MK-STYX reduces stress granules, truncated domains, CH2 (cell division cycle 25 phosphatase homology 2) and DUSP, of MK-STYX were used. Wild-type MK-STYX and the DUSP domain significantly decreased stressed granules that were induced by sodium arsenite, in which G3BP1 (a stress granule nucleator) was used as the marker. In addition, HEK/293 and HeLa cells co-expressing G3BP1-GFP and mCherry-

*Address correspondence to: College of William and Mary, Integrated Science Center, 540 Landrum Drive, Williamsburg, VA, 23185. Tel: 757-221-2587; Fax: 757-221-6483; sdhinton@wm.edu.

Author Contributions

Shantá D. Hinton is responsible for developing the topic, conceptualization of the study, data analysis, as well as training and supervising the graduate student Jonathan Smailys and undergraduates Krystal Fei Jiang, Tatiana Proileau, Kylan Kelley, Simah Nour, and Lina Ali. William J. Buchser is responsible for training the undergraduates Kylan Kelley, Simah Nour, and Lina Ali; Kylan Kelley served as team leader for the quantitative data analysis live cells and the number of stress granules per cell (Figure 4C and D) and provided insightful discussion of the manuscript. In addition, Dr. Buchser parsed and assisted with analyzing the stress granule data for, developed Figure 4 C and D, and provided edits for manuscript. Krystal Fei Jiang performed and analyzed initial experiments that showed that the DUSP domain decreased the number of cells for stress granules (Figure 3) in HEK/293 cells. Titiana Prioleau suggested the inclusion of G3BP1-S149E to demonstrate that wildtype G3BP1 induction of granules is specific for this study, provided fruitful discussion for revision, and edits. In addition, she assisted with the graphical abstract and highlights. Jonathan Smailys and Kylan Kelley (Figure 4E) performed the statistical analysis for these experiments. In addition, Jonathan Smailys performed the co-immunoprecipitated experiments (Figure 5) and assisted with training Olivia Mitchell, who performed the anti-mCherry immunoprecipitation experiments (Figure 5). Jonathan Smailys also performed and analyzed the phosphotyrosine, clone 4G10 (Figure 6), developed the model (Figure 7) and fruitful discussion, editing, and revision of the manuscript. Lynn Zavada assisted with constructs (Figure 1, performed arsenite experiments (Figure 2) and the additional co-transfection experiments with PABP1 (Figures 3 and 4), and training undergraduates Krystal Fei Jiang, Tatiana Prioleau, Kylan Kelley, Olivia Mitchell, and Master's student, Jonathan Smailys. Lynn Zavada also participated in writing the methods, fruitful discussion of data analysis, editing, and revision of the manuscript.

Conflicts of interest

The authors declare that they have no conflicts of interest with the contents of this article.

MK-STYX, mCherry-MK-STYX-CH2, mCherry-MK-STYX-DUSP or mCherry showed that stress granules were significantly decreased in the presence of wild-type MK-STYX and the DUSP domain of MK-STYX. Further characterization of these dynamics in HeLa cells showed that the CH2 domain increased the number of stress granules within a cell, relative to wild-type and DUSP domain of MK-STYX. To further analyze the interaction of G3BP1 and the domains of MK-STYX, coimmunoprecipitation experiments were performed. Cells co-expressing G3BP1-GFP and mCherry, mCherry-MK-STYX, mCherry-MK-STYX-CH2, or mCherry-MK-STYX-DUSP demonstrated that the DUSP domain of MK-STYX interacts with both G3BP1-GFP and endogenous G3BP1, whereas the CH2 domain of MK-STYX did not coimmunoprecipitate with G3BP1. In addition, G3BP1 tyrosine phosphorylation, which is required for stress granule formation, was decreased in the presence of wild-type MK-STYX or the DUSP domain but increased in the presence of CH2. These data highlight a model for how MK-STYX decreases G3BP1-induced stress granules. The DUSP domain of MK-STYX interacts with G3BP1 and negatively alters its tyrosine phosphorylation– decreasing stress granule formation.

Graphical Abstract

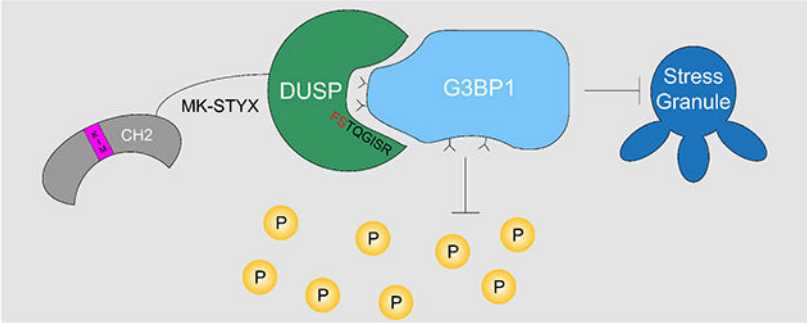

Keywords

MK-STYX; pseudophosphatase; protein tyrosine phosphatase; dual specificity domain; cell division cycle 25 phosphatase homology 2; stress granules; G3BP1

Introduction

The cellular environment endures many aspects of stress such as heat shock, acidity, hypoxia, protein overload, chemical treatment, etc. (1). Cellular survival is dependent on how cells respond to these stressors, and there are many coping mechanisms for cellular stress. Posttranscriptional remodeling, delaying translational initiation, or the degradation of messenger RNA (mRNA) are important examples of how cells manage stress and protect themselves (1).

In addition, messenger RNA (mRNA) may be triaged into mRNA silencing foci termed processing bodies and stress granules (SGs). These membraneless organelles are transiently formed. They may rapidly disassemble under less stressful conditions, allowing the release of mRNA for translation (2). Processing bodies and SGs have very distinctive roles; processing bodies are constitutive and regulate mRNA translation and decay upon a

stimulus. However, SGs are specifically induced by cellular stress such as heat shock, UV irradiation, hypoxia, and sodium arsenite (3,4). They are cytoplasmic storage sites for mRNA that form as a protective mechanism (5,6), and serve as modulators for an equilibrium of apoptosis and cellular survival (2).

SGs accomplish this critical balance through important signaling pathways. The phosphorylation cascade is a major component of this signaling and serves a role in the initial stress response (2). The phosphorylation of the eukaryotic initiation factor 2α (eIF2α) arrests translation and induces SG assembly (6). Therefore, the kinases and phosphatases that control eIF2α phosphorylation maybe critical molecules for regulating SGs. For example, PTEN (phosphatase and tensin homology) (a dual specificity (DUSP) family member) regulates the constitutive phosphatase of eIF2α, CReP (constitutive repressor of eIF2α phosphorylation) (7). The phosphorylation status of RNA biding proteins is a critical regulator of SGs. In particular, the phosphorylation of Ras-GTPase activating protein SH3 domain binding protein-1 (G3BP1), a stress granule nucleator, has been studied extensively. G3BP1 has multiple phosphorylation sites (5). Therefore, multiple sites may be involved in G3BP1's role as an important signaling molecule in stress granule assembly. Initial studies reported that G3BP1 dephosphorylation at Ser-149 was the sole inducer of SG assembly, indicating that the serine at position 149 (Ser-149) was the critical residue that elicits the accumulation of SGs and G3BP1-induced SGs (5). Follow-up studies show that Ser-149 is an important factor in SG assembly (5,8); however, its phosphorylation status may not be the defining factor for it (9). We previously showed that MK-STYX interacts with G3BP1 and decreases the formation of SGs (10). Furthermore, MK-STYX decreases SG formation independently of the phosphorylation status of G3BP1 at serine 149 (11).

The present study focuses on how MK-STYX interacts with G3BP1 to decrease stress granule formation. MK-STYX is a catalytically inactive member of MAPK phosphatase (MKP) subfamily (10,12-17). MKPs possess an N-terminal non-catalytic domain composed of two CDC25 (cell division cycle 25)/rhodanese homology domains and a C-terminal catalytic DUSP domain (15-19). The DUSP domain of MK-STYX does not possess critical histidine and cysteine residues required for catalysis, resulting in its inability to dephosphorylate residues, and therefore it is classified as a pseudophosphatase (14,20). We demonstrate that SGs are significantly decreased in the presence of the DUSP domain of MK-STYX. Intriguingly, we also show that the CH2 domain of MK-STYX increases the number of stress granules within in a cell relative to wild-type MK-STYX and its DUSP domain. In addition, coimmunoprecipitation demonstrated that the DUSP domain of MK-STYX interacts with both endogenous G3BP1 and overexpressed G3BP1. Furthermore, the tyrosine phosphorylation of G3BP1 is increased in the presence of the CH2 domain, but decreased in the presence of MK-STYX and the DUSP domain. Taken together these data provide a platform of how MK-STYX may interact with G3BP1 to decrease stress granules–serving as the framework to understanding the mechanism. Our findings highlight that pseudophosphatase MK-STYX decreases SGs through its DUSP domain. Moreover, this specificity demonstrates that the DUSP domain is very important for protein interaction and function of this pseudophosphatase as a regulator in the stress response pathway.

Results

The DUSP domain of MK-STYX inhibits endogenous G3BP1 stress granules

To determine how MK-STYX decreases stress granules, we investigated whether its CH2 domain, DUSP domain, or both domains are required for its effects on stress granules. We used wild-type MK-STYX and truncated mutants (Figure 1) to determine whether MK-STYX decreases stress granules. The CH2 domain consists of residues 1-150, which contains the kinase interaction motif (KIM) (Figure 1B) and is referred to as MK-STYX-CH2 (Figure 1B). The DUSP domain consists of residues 151-313 (Figure 1C) and is referred to as MK-STYX-DUSP (Figure 1C). The protein tyrosine phosphatase (PTP) active signature motif (HCX_5R), which is essential for catalysis, is within this region. However, the HC is replaced with FS in MK-STYX (Figure 1A and 1C) (16,17,20).

The assembly of stress granules is triggered following stimulation of cells with arsenite (5). This process can be visualized by the change in intracellular localization of endogenous G3BP1 from a diffuse distribution throughout the cytoplasm to the large stress granule structures. To test whether each domain of MK-STYX could affect this process, we compared the effects of arsenite on localization of endogenous G3BP1 in both HEK/293 cells and HeLa cells transfected with mCherry-MK-STYX, mCherry-MK-STYX-CH2 or mCherry-MK-STYX-DUSP. These two different cell types were chosen both to avoid any cell line bias in our present study of the interaction and because they had been used previously by others (2,3) and our initial studies of G3BP1 (10). To determine whether the effects of MK-STYX was solely on G3BP1 induced stress granules, the poly (A)-binding protein 1 (PABP1), which is another marker for stress granules (3,21), was also visualized. The expression of endogenous G3BP1 was visualized by staining with anti-G3BP1 and FITC-conjugated secondary antibody and analyzed by fluorescence microscopy (Figure 1). Exposure to arsenite induced stress granule formation, which was determined by G3BP1 accumulation) in approximately 87% (HEK/293) (Figure 2A and D) or 75% (HeLa) (Figure 2B and E) of control (mCherry expressing) cells, whereas expression of MK-STYX resulted in a significant ($p < 0.05$) decrease in stress granule formation; only approximately 54% ($p < 0.005$) of HEK/293 or 60% ($p < 0.05$) of HeLA cells transfected with the MK-STYX expression plasmid formed stress granules (Figure 2). Furthermore, the cells expressing DUSP demonstrated a similar pattern as wildtype MK-STYX, decreasing the SGs (Figure 2).

The expression of G3BP1 was used to score the cells for SGs; however, the poly (A)-binding protein 1 (PABP1) was impacted by cells expressing MK-STYX and DUSP plasmids. PABP1 is cytoplasmic in non-stressful conditions; however, it locates to the stress granules or nucleus under stressful conditions such as UV, heat shock, or arsenite stress (21). When stressed cells are in a recovery stage, in which mRNA can be inhibited from translation, PABP1 locates to the nucleus to protect mRNAs. In contrast, when stressed cells are in a toxic stage, the PABP1 forms stress granules (21). These studies show that PABP1 is cytosolic in non-stressed HEK/293 cells (Figure 2A) and whole cell in HeLa cells (Figure 2D). In both arsenic stressed HEK/293 and HeLa cells PABP1 became mostly nuclear with SG starting to form in the presence of mCherry and mCherry-MK-STYX-CH2 expressing

plasmids (2B and E), indicating cells are beginning to exit the recovery period. Furthermore, HeLa, cells that were near dying or becoming toxic consisted of more pronounced PABP1 SGs, which overlapped with G3BP1 SGs (Figure 2 PABP1 granules).

The DUSP domain of MK-STYX inhibits G3BP1-induced stress granules

Stress granule formation has also been shown to be induced by overexpression of G3BP1 alone (5). Therefore, we tested whether expression of wild-type MK-STYX, CH2, or DUSP affected stress granule formation by excess G3BP1. G3BP1-GFP and mCherry-MK-STYX, mCherry-MK-STYX-CH2 or mCherry-MK-STYX-DUSP were ectopically expressed in both HEK/293 and HeLa cells. As anticipated from our previous reports with pMT2-FLAG-MK-STYX-FLAG and pMT2-FLAG-MK-STYX$_{active}$-FLAG mammalian expression constructs (10,11), wild-type MK-STYX resulted in a significant decrease in cells expressing stress granules in both HEK/293 (Figure 3) and HeLa (Figure 4) cells. The overexpressed G3BP1-GFP was diffuse through the cell instead of in the hallmark accumulation of aggregates, which form in the presence of G3BP1-GFP. Cells co-expressing GFP and mCherry or mCherry-MK-STYX constructs significantly decreased the number of granules (Figure 3B and 4B). Thus, cells expressing GFP and mCherry served as the control in a comparison for cells expressing G3BP1-GFP and mCherry-MK-STYX constructs (Figures 3A and 4A). To validate further that it is wild-type G3BP1-GFP that induces granules, G3BP1-S149E-GFP, represented as G3BP1 149E in figures, was used as a negative control. Cells expressing G3BP1-S149E-GFP have been reported to dramatically decrease stress granules (11). Dephosphorylation of serine 149 was initially reported as the only residue essential for stress granule assembly. The G3BP1-S149E mimics, which mimic phosphorylation, were a critical component of these studies (5). Cells were scored for granules, and these data were analyzed for statistical analysis (Figures 3B and 4B). G3BP-1-GFP was used to score cells with granules. The PABP1 did not show pronounced granules, but they were distributed between cytosolic and nuclear compartments. Because these cells were not stressed with arsenite, these results are rationale and align with previous studies of the localization of PABP1. HeLa cells heat shocked and probed for PABP1 as a stress granule marker did not accumulate stress granules; only cells treated with arsenite formed stress granules (21). There was a significant ($p < 0.005$) difference between the cells co-expressing G3BP1-GFP and mCherry in HEK/293 (~62%) and HeLa (~58%) and cells co-expressing G3BP1-GFP or mCherry-MK-STYX (~42% in HEK/293 and ~24% in HeLa) or mCherry-MK-STYX-DUSP (~34% in HEK/293 and ~29% in HeLa) (Figure 3B and 4B, respectively), indicating that it is the DUSP domain of MK-STYX that is responsible for decreasing stress granules. Intriguingly, cells expressing G3BP1-GFP and mCherry-MK-STYX-CH2 (~59% in HEK/293 and ~60% HeLa) appeared to form stress granules (Figure 3B and 4B) similar to cells co-expressing G3BP1 and mCherry for both HEK/293 (~62%) and HeLa (~58%).

Cells expressing G3BP1-GFP and mCherry-MK-STYX-CH2 appeared to form SG similar to cells expressing G3BP1-GFP and mCherry; however, these granules appeared phenotypically different. We characterized cells with SG formation for all conditions. To ascertain whether G3BP1 displayed a different distribution throughout the cytoplasm to form stress granule organelles, large, small, or dispersed G3BP1-GFP, we compared the

effects of mCherry-MK-STYX, mCherry-MK-STYX-CH2, and mCherry-MK-STYX-DUSP on G3BP1 induced SG in HeLa cells (Figure 4C and D). These cells were chosen because they were used in our (10,11) and other previous studies for characterization of granules (5); Tourriere et al used them and Cos-7 in the initial studies with G3BP1-GFP (5). It is important to note that studies performed to obtain data analyzed in Figures 2, 3, and 4A and B scored all cells whether granules formed or not. However, to determine whether G3BP1 displayed a different distribution throughout the cytoplasm to form stress granule organelles, large, small, or dispersed G3BP1-GFP, only cells expressing stress granules could be appropriately analyzed to address this question and obtain data. Characterization of cells that only displayed stress granules showed that granules in the presence of G3BP1-GFP and mCherry-MK-STYX (WT) or mCherry-MK-STYX-DUSP formed typical large perinuclear G3BP1-GFP induced granules (Figure 4C). Whereas the stress granules in the presence of G3BP1-GFP and mCherry or mCherry-MK-STYX-CH2 were dispersed throughout cells. Furthermore, mCherry-MK-STYX-CH2 significantly increased the number of stress granules per cell compared to wild-type mCherry-MK-STYX or mCherry-MK-STYX-DUSP (Figure 4D). This indicates that each domain of MK-STYX may affect the accumulation of G3BP1-GFP independently of altering its (CH2 or DUSP) role on G3BP1-GFP to form (or not form) granules, respectively. The domains together do not affect the expression of G3BP1-GFP to decrease SG; we previously reported that MK-STYX does not affect the expression of G3BP1 (10). This variation of the number of stress granules in cells in the presence of wild-type MK-STYX or DUSP domain and CH2 domain provides more avenues to explore how MK-STYX decreases SGs.

The DUSP domain interacts with G3BP1

To determine how MK-STYX and G3BP1 interact, we co-transfected HEK/293 cells with expression vectors for GFP or GFP-tagged G3BP1 and either mCherry tagged MK-STYX, the CH2 domain of MK-STYX, or its DUSP domain. The initial interaction and mass spectrometry study that identified MK-STYX and G3BP1 as binding partners was performed in HEK/293s (10). We immunoprecipitated G3BP1 with anti-G3BP antibodies and observed, by immunoblotting with mCherry antibodies, that wild-type MK-STYX or MK-STYX-DUSP co-precipitated with G3BP1 (Figure 5). The CH2 domain of MK-STYX did not co-precipitate with G3BP1 (Figure 5). Furthermore, it appeared that more MK-STYX-DUSP co-precipitated than the wild-type MK-STYX (Figure 5A; low expression and 5B). This strong binding of the DUSP domain (47kD) was also observed in the reciprocal experiment, which we immunoprecipitated with anti-mCherry antibodies (Figure 5A) and immunoblotted for the presence of G3BP1 (Figure 5B). Immunoprecipitation assays are sensitive and there could have been a blockage of the binding site by antibody and/or a different folding between wild-type MK-STYX and the DUSP domain, which is why the reciprocal study did not demonstrate an interaction between G3BP1 and wild-type mCherry-MK-STYX when immunoprecipitated with mCherry antibodies. Nevertheless, the DUSP domain of MK-STYX bound with G3BP1 (both endogenously and ectopically expressed in both co-immunoprecipitation experiments), whereas the CH2 domain did not (Figure 5A-B). Taken together, these experiments demonstrate that MK-STYX and G3BP1 interact through the DUSP domain of MK-STYX, to decrease stress granules. Furthermore, each domain

of MK-STYX has a distinct function similar to those of its active homologs, MKPs, of MK-STYX (15,16,18,19).

G3BP1 tyrosine phosphorylation is increased in the presence of the CH2 domain of MK-STYX

Because G3BP1 has several phosphorylation sites and MK-STYX is a member of the protein tyrosine phosphatase family, obtaining a phosphotyrosyl profile of proteins in the presence of MK-STYX and its domain would help us understand the function of MK-STYX. Thus, tyrosine phosphorylation assays were performed (Figure 6A). The immunoblots of HEK/293 cells coexpressing GFP or GFP-tagged G3BP1 and either mCherry-tagged MK-STYX, CH2 domain of MK-STYX, or DUSP domain of MK-STYX demonstrated a change in the tyrosine phosphorylation pattern of proteins at ~ 75 Kd, 37 Kd, and higher molecular weight proteins, which are labeled with black arrows for ECL and Merged images (Figure 6A). No-Stain (Invitrogen, Thermofisher) was used to assure normalization of the total protein in the lysate samples. The changes of the tyrosine phosphorylation of several proteins between the wild-type MK-STYX, CH2, or DUSP indicates that MK-STYX has a role in the phosphorylation signaling cascade–serving as a platform for future studies to identify these molecules.

Phosphorylation of G3BP1 at tyrosine 40 (Y-40) was recently reported to be essential for the formation of SG (22). To determine whether MK-STYX, CH2, or DUSP affects the tyrosine phosphorylation of G3BP1, the immunoprecipitated G3BP1 was analyzed for tyrosine phosphorylation. Immunoblots of the IP with G3BP1 antibodies were probed with anti-phosphotyrosine, clone 4G10 (pY4G10) antibodies. The tyrosine phosphorylation of G3BP1 increased in the presence of CH2 (Figure 6B) but not in the presence of DUSP (Figure 6B). G3BP1 tyrosine phosphorylation is required for SG formation (22); therefore, its increased tyrosine phosphorylation in the presence of the CH2 domain, which increases SG, was expected, and supports the other data presented. G3BP1 tyrosine phosphorylation is not altered in the presence of the DUSP domain– suggesting that the mechanism that MK-STYX uses to reduces SG is through regulating the tyrosine phosphorylation of G3BP1.

Discussion

MK-STYX is a pseudophosphatase member of the PTP family (10,20,23,24). Pseudophosphatases have emerged as key regulators in signal transduction cascades by serving as competitors, signaling integrators, modulators, and anchors in cellular processes (14,16,24,25). These molecules are perceived as enzymatically inactive due to mutations of critical residues important to their catalytic function (14,16,17,23-25), but may maintain a three-dimensional fold (14,20,24,26,27). In particular, pseudophosphatases of the PTP family have mutations within their signature active site motif (HCX_5R) that render them inactive (14,16,17,23-25,27). Focused attention on investigating pseudophosphatases has resulted in better understanding of these molecules as important players in physiology and pathophysiology, revealing their roles in diseases (24,25,28). Thus, their dysregulation may result in various diseases such as diabetes, cancer, neurological diseases, etc. (25,28).

Over the past two decades, we have investigated the pseudophosphatase MK-STYX, which is a regulator in the cellular stress response, apoptosis, and neuronal differentiation (24,28-34). In addition, MK-STYX has been shown to alter the localization of histones and change the post-translational modifications of tubulin (35). Evolutionary computational analysis demonstrates that MK-STYX diverges from its active MKP homologs (36); this plasticity may explain its roles in numerous pathways (36). There have been significant contributions to understanding MK-STYX as a signal regulator. However, the molecular mechanism, which is a major goal of the pseudoenzyme fields, remains elusive. This study serves an important framework towards elucidating the molecular mechanism for MK-STYX in the stress response pathway. We demonstrate that the DUSP domain interacts with G3BP1 and significantly decreases stress granules. In addition, we demonstrate that the CH2 domain of MK-STYX significantly increases the number of stress granules within a cell. Taken together this demonstrates that each domain of MK-STYX has very distinct functions such as its active MKP homologs, where the CH2 domains serve as a docking domain for MAPKs to assist in efficient catalysis by the DUSP domain (15,18,19). Moreover, these data serve as the initial platform to understand the intricate role of MK-STYX in regulating stress granules.

G3BP1 is a stress granule nucleator (10,37,38). It is a 52 kDa (resolving at 68 kDa) (5,10,39) protein that is ubiquitously expressed and contains several distinct domains that enable it to interact with multiple protein and RNA binding partners (40,41). Several studies with G3BP1and phosphorylated mutants have revealed important insights into the dynamic assembly of stress granules (3,5,29,42,43). G3BP1 has many residues that may be phosphorylated and play a critical role in SG assembly (10). For example, our previous studies revealed that MK-STYX decreases the phosphorylation state of serine 149. Furthermore, a more recent report highlights key residues and structural dynamics of G3BP1 that are critical for its ability to serve as a hub for a multicomplex with cytosolic phosphoproteins (39). Mutations of G3BP1 resulted in less affinity to binding partners USP10 and Caprin 1 (39). The specificity of G3BP1 to bind the DUSP domain of MK-STYX but not the CH2 domain supports the selectivity of G3BP1 as an intrinsically disorder protein capable of forming homotypic and heterotypic complexes.

The non-catalytic N-terminal CH2 domains serve as docking domains for the substrate specificity of MAPKs (15-19,23). This study shows that the DUSP serves as the docking domain for G3BP1. Reports have shown that MK-STYX does not regulate ERK/MAPK phosphorylation (16,17,31). Bioinformatic analysis of MK-STYX demonstrates that it also has mutations within the KIM motif of the CH2 domain (16,17), preventing MAPK/ERK from interacting at this domain (16). However, the prototypical pseudophosphatase STYX has only a DUSP domain, to which ERK1/2 binds (25,44). Thus, the pseudophosphatase “STYX” domains may serve as docking domains and as signaling regulators. Furthermore, in this study the DUSP domain serves as a docking domain for G3BP1.

Considering that the CH2 domain increases the number of cells that form stress granules and significantly increases the number of stress granules within a cell, it may interact with other molecules such as RNA or RNA binding proteins (RBPs) in addition to, instead of G3BP1. The PABP1 redistribution to the nucleus in the presence of MK-STYX constructs supports

such a possibility. Under stressful conditions PABP1 locates to the nucleus and interacts with mRNA to regulate RNA stability and translation for cell recovery; PABP1 localization to the nucleus prevents RNA transport (21). This could explain the effects of wild-type MK-STYX and truncated DUSP on decreasing stress granule assembly. Furthermore, the DUSP domain may bind G3BP1, preventing it from serving as the hub for a multicomplex of RNAs and RNA binding proteins. Such proteins may bind the CH2 domain independently of G3BP1 to form stress granules; stress granules consist of many molecules and do not always include G3BP1 (2). However, G3BP1 induces more smaller granules. We previously showed that wild-type MK-STYX interacts with G3BP1 and decreases stress granules (10), as confirmed in the present study. This implies that the function of the DUSP domain role in stress granule assemblies suppresses the action of the CH2 domain when full length MK-STYX folds.

This study is a significant contribution to a potential model by which MK-STYX interacts with G3BP1 to decrease stress granules (Figure 7). Intriguingly, a recent report identified a protein tyrosine kinase, Bruton's tyrosine kinase (BTK), as an essential signaling regulator of G3BP1 induced stress granules (22). The N-terminus of the G3BP1 consists of a NTF (nuclear transport factor) 2-like domain and a segment rich in acidic residues. The central segment contains proline-rich PXXP motifs, and the C-terminal portion of the protein contains an arginine- and glycine-rich RGG box, which recognizes and binds RNA binding proteins (45) (Figure 7A). Furthermore, truncated NTF and/or RGG drastically alters the formation of stress granules (5). BTK binds G3BP1 and phosphorylates its tyrosine residue at position 40, which is located in the NTF-like domain, to induce stress granule aggregates under stressful conditions (22) (Figure 7A). This is a major finding demonstrating that G3BP1's tyrosine phosphorylation status is critical in regulating the formation of stress granules (22). Furthermore, tyrosine phosphorylation by BTK shows that a PTP is involved in stress granule formation. Interestingly, this study demonstrates that a non-catalytically active member of PTPs uses its DUSP domain to interact with G3BP1 and decreases stress granules. Perhaps, MK-STYX binds G3BP1 through its DUSP domain, blocking the action of BTK and preventing stress granule formation (Figure 7B). The existence of several phosphorylated residues of G3BP1 indicate that there may be other PTPs involved in the stress granule life cycle; an active homolog (MKP) of MK-STYX has been shown to induce SG (unpublished data).

The expression of G3BP1 is increased in tumors [34]. Furthermore, the phosphorylation of G3BP1 has resulted in tumors and cancer [33], revealing the importance of understanding proteins of the phosphorylation cascade that interacts with G3BP1 and positively or negatively regulates stress granules. Since it is the tyrosine phosphorylation that positively regulates the formation of stress granules, it will be insightful to understands the impact of proteins that are involved in dephosphorylating and/or negatively regulating the formation of stress granules. Intriguingly, the phosphorylation of G3BP1 at Ser-149 by casein kinase 2α triggers granule disassembly, releasing axonal mRNAs to participate in axonal growth (46). We previously reported that MK-STYX induces neurite outgrowths in PC12 cells (29,34). In addition, MK-STYX alters the morphology of hippocampal primary neurons in rats. The axons and dendrites are not visually distinctive, and there is an increase in the number of neurites (33).

Stress granules are transient structures, but when prolonged may become toxic, resulting in neurodegeneration (2,47,48). G3BP1 phosphorylation is crucial regardless of whether stress granules form (phosphorylation at tyrosine 40) (22) or disassemble (phosphorylation at serine 149) (46). This linkage between MK-STYX and stress granules through tyrosine phosphorylation of G3BP1 and that MK-STYX induces neurites is exciting. It validates the continued pursuit of studying the dynamic between MK-STYX and G3BP1 and further investigation of this pseudophosphatase. For instance, MK-STYX has been implicated in aggregates beyond SGs such as aggresomes (49), accumulation of misfolded protein. These studies show that in HEK/293 cells expressing wild-type MK-STYX or the DUSP domain forms aggregates that also resemble aggresomes (Figure 2A-B and Figure 3) – providing other avenues to study MK-STYX.

The pseudophosphatase MK-STYX has always provided complexity to the phosphorylation cascade and the life cycle of stress granules. Our key finding is that the DUSP domain of MK-STYX is responsible for its interaction with G3BP1. This interaction inhibits SG formation and so introduces a new level of nuance to the multifaceted and complex phenomenon of stress granules.

Experimental Procedures

Plasmid constructs

pmCherry-MK-STYX, pmCherry-MK-STYX-CH2, pmCherryMK-STYX-DUSP, and pmCherry-MK-STYX$_{(\text{active mutant})}$ encode functional, N-terminal red fluorescent protein (mCherry)-tagged human MK-STYX fusion protein. cDNAs for the truncated CH2 domain (CH-2-MK-STYX), and DUSP domain (MK-STYX-DUSP) were synthesized by Invitrogen GeneArt Gene Synthesis (ThermoFisher Scientific), and subcloned into mCherry-C1 vectors (N-terminal tag, Clontech Laboratories, Inc.). The integrity of all constructs derived from PCR was confirmed by DNA sequencing. pGFP was purchased from Clontech Laboratories. The G3BP1-GFP constructs were kindly provided by Jamai Tazi (Institut de Génétique Moléculaire, France) and previously used (10).

Antibodies

The following antibodies were used: Anti-G3BP antibody (BD 611127 2); anti-GFP antibody (ThermoFisher; MA5-15256); anti-mCherry antibody (SAB2702291); antiPABP-Cy5 (Bioss BS-3836R-Cy5 antibody; anti-mouse-FITC antibody (Abcam AB6785)). (ThermoFisher; anti-phosphotyrosine, clone 4G10 (Millipore; 05-321); and anti- beta tubulin polyclonal antibody (ThermoFisher; PA1-21153).

Cell culture and transient transfection

HEK/293 (ATCC) cells were maintained at 37°C, 5% CO_2 Dulbecco's Modified Eagle medium (DMEM, Invitrogen) supplemented with 10% fetal bovine serum (FBS). Transfections were performed using Lipofectamine 2000 Reagent (Invitrogen); cells were transfected with expression plasmids pGFP, GFP-G3BP1, mCherry, mCherry-MK-STYX, mCherry-MK-STYX-CH2, or mCherry-MK-STYX-DUSP. Cells were analyzed by fluorescence microscopy, immunoprecipitation and/or immunoblotting.

For experiments examining the effect of MK-STYX on stress-induced stress granule formation, at 23 h post-transfection, HeLa cells were treated with 500 μM sodium arsenite (Sigma Millipore 1.062777) for 30 minutes, then processed as above. To visualize stress granule formation, endogenous G3BP1was used as the marker and visualized with anti-G3BP and FITC - conjugated goat anti-mouse Zymed Laboratories) antibodies. In addition, PABP1 was used as a marker and visualized with anti-PABP1-conjugated to Cy5. The normal goat serum was purchased from Invitrogen (31872).

Transient transfection and cell imaging

For immunofluorescence assays, HEK/293 or HeLa cells were grown to 80-90% confluence and 2 X 10^5 cells were plated onto glass coverslips in 6-well dishes (Nunc). Twelve to eighteen hr post-plating, cells at 40-60% confluence were co-transfected with 2 μg of pGFP or pGFP-G3BP1 and mCherry, mCherry-MK-STYX, mCherry-MK-STYX-CH2 or mCherry-MK-STYX-DUSP expression plasmid DNA and 4 μl of Lipofectamine 2000 Reagent (Invitrogen) per well, according to the manufacturer's protocol. The medium was replaced 5 hr after transfection. Twenty-four hr post-transfection, cells were washed with PBS and fixed with 3.7% formaldehyde. The coverslips were mounted to a slide using GelMount containing 4′, 6-diamidino-2′-phenylinodole dihydrochloride (DAPI, Sigma) (0.5 mg/ml). Coverslips used for HEK/293 cells were treated with Poly-D-Lysine according to the Invitrogen Poly-D-Lysine Solution protocol.

Cells were scored for stress granule assembly, which forms when G3BP1-GFP is overexpressed (5). Samples were scored blind with regard to treatment and were scored independently by two different individuals. Cells were scored into two categories: no stress granules and stress granules. At least three replicate transfections were performed and approximately 100 cells were scored per replicate. Counting and image collection were performed on a Nikon ECLIPSE Ti inverted fluorescence microscope. NIS-Elements Basic Research software (version 5.21.02) was used for image acquisition and primary image processing, and Adobe Photoshop, and Illustrator were used for secondary image processing.

Stress granule automated live cell imaging and quantitation

HeLa cells were grown to 80-90% confluence and 2 X 10^5 cells were plated onto 6-well dishes (Nunc). Twelve to eighteen hours post-plating, cells at 40-60% confluence were co-transfected with 2 μg of pGFP or pGFP-G3BP1 and mCherry, mCherry-MK-STYX, mCherry-MK-STYX-CH2 or mCherry-MK-STYX-DUSP expression plasmid DNA and 3 μl of Lipofectamine 2000 Reagent (Invitrogen) per condition/well, according to the manufacturer's protocol. Six-hour post-transfection, cells were seeded onto 96 well-plates using the Biomek i5 Automated Workstation.

Eighteen hours post-seeding, cells were stained with Hoecsht nuclear stain (1:1000) and analyzed by confocal microscopy. Only cells expressing stress granules were analyzed and imaged for all conditions, with each condition represented in eight replicate wells and ~250 cells counted. A Cytiva INCell 6500 HS Confocal microscope with a 20x 0.45 NA objective was used. Three channels (Hoechst, GFP, mCherry) and 30 fields per well were imaged.

Incarta was used for cell tracing and secondary image processing, followed by analysis with Spotfire, big data software for quantification. The Laser Autofocus Module was used during the experiment. Data from eight biologically independent replicate wells were recorded.

Immunoblotting

HEK/293 cells were transfected with pGFP, pGFP-G3BP1, mCherry, mCherry-MK-STYX, mCherry-MK-STYX-CH2, or mCherry-MK-STYX-DUSP expression plasmids, lysed, and analyzed by western blotting. Cells were harvested in lysis buffer (50 mM HEPES, pH 7.2, 150 mM NaCl, 10% glycerol, 10 mM NaF, 1 mM Na_3VO_4, 1% Nonidet P-40 alternative [Calbiochem], phosphotablet (Roche) and protease inhibitor cocktail tablets [Roche]). Lysates were sonicated, centrifuged at 14,000 X g for 10 min, and the supernatant protein concentration was determined by NanoDrop quantification. Lysates were resolved by 10% SDS-PAGE and transferred to PVDF membrane by TransBlot (Biorad) for immunoblot analysis with anti-G3BP1, anti-GFP; anti-mCherry antibody; anti-phosphotyrosine, clone 4G10; anti- beta tubulin polyclonal antibodies, followed by chemiluminescent detection. No-Stain labeling reagent (Invitrogen-ThermoFisher; A44449) was used to visualize, normalize, and/or quantify proteins. When warranted, blots were stripped (200 mM glycine, 3.5 mM SDS, 1% Tween 20), and re-probed.

Immunoprecipitation and Immunoblotting

Forty-eight hours post-transfection, HEK/293 cells were harvested in lysis buffer (50 mM HEPES, pH 7.2, 150 mM NaCl, 10% glycerol, 10 mM NaF, 1% Nonidet P-40 alternative [Calbiochem], and protease inhibitor cocktail tablets (Roche). Lysates were centrifuged at 14,000 X g for 10 min, and the supernatant protein concentration was determined by Pierce 660nm Protein Assay Reagent. For immunoprecipitation, the lysates were precleared, and incubated with anti-G3BP (Sigma) or anti-mCherry (Thermo) for 1 h at 4°C, followed by incubation with Protein G beads (GE Healthcare). Samples were washed three times in lysis buffer and boiled in Laemmli sample buffer. Lysates were resolved by 10% SDS-PAGE and transferred to a PVDF membrane (GE Healthcare) for immunoblot analysis with anti-G3BP (BD Bioscience), anti-mCherry, anti-GFP, anti-phosphotyrosine, clone 4G10, or anti- β tubulin (ThermoFisher) antibodies, followed by chemiluminescent detection with the iBright Imager FL-500 (Invitrogen).

Statistical Analysis

Analysis of variance (ANOVA) was used to compare all samples to each other. To further determine the statistical significance of differences between cells not expressing and expressing stress granules Tukey's post-hoc analysis was applied to determine significance between groups, where a $p < 0.05$ was considered statistically significant. All data are expressed as mean ± SD. ANOVA and Tukey's post-hoc test also was used to determine significant differences for the quantitative analysis of stress granules of each condition.

Acknowledgements

We thank Dr. Jamai Tazi (Institut de Génétique Moléculaire, France) for the G3BP1 construct. We are grateful to Dr. Lizabeth A. Allison for her continued support and Vincent Roggero assistance with constructs and formatting figures. We also thank Dr. William R. Eckberg for editing our work.

Funding

Funding for this work was funded by the National Science Foundation (NSF) MCB 1909316 awarded to S. D. H and the National Institute of Health (NIH): NIH Research 1 R15 NS115074-1 to S.D.H.; Charles Center Summer Research Grants to T.P (2020 and 2021) and K.K. (2020 and 2021) and at the College of William and Mary.

Data Availability

The data that support the findings in this manuscript are available from the corresponding author upon request.

Abbreviations

BTK	Bruton's tyrosine kinase
CH2	cell division cycle 25 phosphatase homology 2
CReP	constitutive repressor of eIF2α phosphorylation
DNA	deoxyribonucleic acid
DUSP	dual-specificity phosphatase or the dual-specificity phosphatase domain
eIF2α	eukaryotic initiation factor 2 alpha
ERK	extracellular signal-regulated kinases ½
G3BP1	Ras-GTPase activating protein SH3 domain binding protein-1
GFP	green fluorescent protein
IB	immunoblotting
IDR1/3	intrinsically disordered region 1/3
IP	immunoprecipitated
KIM	kinase interaction motif
MAPK	mitogen-activated protein kinase
mCherry	monoclonal Cherry
MEK	mitogen-activated protein kinase kinase
MM/GBSA	molecular mechanics generalized Born surface area
MKP#	MAP kinase phosphatase with an assigned number
MK-STYX	mitogen-activated protein kinase phosphoserine/threonine/tyrosine-binding protein
mRNA	messenger ribonucleic acid
PABP1	poly (A)-binding protein 1

pERK	phospho-ERK
pSer	phospho-serine
pThr	phospho-threonine
pTyr	phospho-tyrosine
PTEN	phosphatase and tensin homology
PTP	protein tyrosine phosphatase
PTPM1	PTP localized to the mitochondrion
RCSB	Research Collaboratory for Structural Bioinformatics
SD	standard deviation
STYX	phosphoserine/threonine/tyrosine-interacting protein
STYXL1	STYX-like-1
SG	stress granules
ssRNA	single stranded RNA
TIA-1	T-cell intracellular antigen-1

References

1. Ron D. (2006) Cell biology. Stressed cells cope with protein overload. Science 313, 52–53 [PubMed: 16825557]
2. Thomas MG, Loschi M, Desbats MA, and Boccaccio GL (2011) RNA granules: the good, the bad and the ugly. Cellular signalling 23, 324–334 [PubMed: 20813183]
3. Kedersha N, Stoecklin G, Ayodele M, Yacono P, Lykke-Andersen J, Fritzler MJ, Scheuner D, Kaufman RJ, Golan DE, and Anderson P (2005) Stress granules and processing bodies are dynamically linked sites of mRNP remodeling. The Journal of cell biology 169, 871–884 [PubMed: 15967811]
4. Tourriere H, Chebli K, and Tazi J (2002) mRNA degradation machines in eukaryotic cells. Biochimie 84, 821–837 [PubMed: 12457569]
5. Tourriere H, Chebli K, Zekri L, Courselaud B, Blanchard JM, Bertrand E, and Tazi J (2003) The RasGAP-associated endoribonuclease G3BP assembles stress granules. The Journal of cell biology 160, 823–831 [PubMed: 12642610]
6. Kedersha NL, Gupta M, Li W, Miller I, and Anderson P (1999) RNA-binding proteins TIA-1 and TIAR link the phosphorylation of eIF-2 alpha to the assembly of mammalian stress granules. The Journal of cell biology 147, 1431–1442 [PubMed: 10613902]
7. Zeng N, Li Y, He L, Xu X, Galicia V, Deng C, and Stiles BL (2011) Adaptive Basal Phosphorylation of eIF2alpha Is Responsible for Resistance to Cellular Stress-Induced Cell Death in Pten-Null Hepatocytes. Mol Cancer Res
8. Tourriere H, and Tazi J (2019) Reply to “Phosphorylation of G3BP1-S149 does not influence stress granule assembly”. The Journal of cell biology 218, 2433–2434 [PubMed: 31171633]
9. Panas MD, Kedersha N, Schulte T, Branca RM, Ivanov P, and Anderson P (2019) Phosphorylation of G3BP1-S149 does not influence stress granule assembly. The Journal of cell biology 218, 2425–2432 [PubMed: 31171631]

10. Hinton SD, Myers MP, Roggero VR, Allison LA, and Tonks NK (2010) The pseudophosphatase MK-STYX interacts with G3BP and decreases stress granule formation. The Biochemical journal 427, 349–357 [PubMed: 20180778]
11. Barr JE, Munyikwa MR, Frazier EA, and Hinton SD (2013) The pseudophosphatase MK-STYX inhibits stress granule assembly independently of Ser149 phosphorylation of G3BP-1. The FEBS journal 280, 273–284 [PubMed: 23163895]
12. Caunt CJ, and Keyse SM (2013) Dual-specificity MAP kinase phosphatases (MKPs): shaping the outcome of MAP kinase signalling. The FEBS journal 280, 489–504 [PubMed: 22812510]
13. Wishart MJ, Denu JM, Williams JA, and Dixon JE (1995) A single mutation converts a novel phosphotyrosine binding domain into a dual-specificity phosphatase. The Journal of biological chemistry 270, 26782–26785 [PubMed: 7592916]
14. Hinton SD (2019) The role of pseudophosphatases as signaling regulators. Biochimica et biophysica acta. Molecular cell research 1866, 167–174 [PubMed: 30077638]
15. Dickinson RJ, and Keyse SM (2006) Diverse physiological functions for dual-specificity MAP kinase phosphatases. Journal of cell science 119, 4607–4615 [PubMed: 17093265]
16. Hepworth EMW, and Hinton SD (2021) Pseudophosphatases as Regulators of MAPK Signaling. International journal of molecular sciences 22
17. Hinton SD (2020) Pseudophosphatase MK-STYX: the atypical member of the MAP kinase phosphatases. The FEBS journal 287, 4221–4231 [PubMed: 32472731]
18. Keyse SM, and Ginsburg M (1993) Amino acid sequence similarity between CL100, a dual-specificity MAP kinase phosphatase and cdc25. Trends in biochemical sciences 18, 377–378 [PubMed: 8256285]
19. Bordo D, and Bork P (2002) The rhodanese/Cdc25 phosphatase superfamily. Sequence-structure-function relations. EMBO reports 3, 741–746 [PubMed: 12151332]
20. Wishart MJ, and Dixon JE (1998) Gathering STYX: phosphatase-like form predicts functions for unique protein-interaction domains. Trends in biochemical sciences 23, 301–306 [PubMed: 9757831]
21. Burgess HM, and Gray NK (2012) An integrated model for the nucleo-cytoplasmic transport of cytoplasmic poly(A)-binding proteins. Commun Integr Biol 5, 243–247 [PubMed: 22896784]
22. Kim SS, Sim DCN, Carissimo G, Lim HH, and Lam KP (2022) Bruton's tyrosine kinase phosphorylates scaffolding and RNA-binding protein G3BP1 to induce stress granule aggregation during host sensing of foreign ribonucleic acids. The Journal of biological chemistry 298, 102231 [PubMed: 35798143]
23. Tonks NK (2013) Protein tyrosine phosphatases--from housekeeping enzymes to master regulators of signal transduction. The FEBS journal 280, 346–378 [PubMed: 23176256]
24. Reiterer V, Pawlowski K, Desrochers G, Pause A, Sharpe HJ, and Farhan H (2020) The dead phosphatases society: a review of the emerging roles of pseudophosphatases. The FEBS journal 287, 4198–4220 [PubMed: 32484316]
25. Reiterer V, Eyers PA, and Farhan H (2014) Day of the dead: pseudokinases and pseudophosphatases in physiology and disease. Trends in cell biology 24, 489–505 [PubMed: 24818526]
26. Todd AE, Orengo CA, and Thornton JM (2002) Sequence and structural differences between enzyme and nonenzyme homologs. Structure 10, 1435–1451 [PubMed: 12377129]
27. Tonks NK (2009) Pseudophosphatases: grab and hold on. Cell 139, 464–465 [PubMed: 19879835]
28. Mattei AM, Smailys JD, Hepworth EMW, and Hinton SD (2021) The Roles of Pseudophosphatases in Disease. International journal of molecular sciences 22
29. Flowers BM, Rusnak LE, Wong KE, Banks DA, Munyikwa MR, McFarland AG, and Hinton SD (2014) The pseudophosphatase MK-STYX induces neurite-like outgrowths in PC12 cells. PloS one 9, e114535 [PubMed: 25479605]
30. Niemi NM, Sacoman JL, Westrate LM, Gaither LA, Lanning NJ, Martin KR, and MacKeigan JP (2014) The pseudophosphatase MK-STYX physically and genetically interacts with the mitochondrial phosphatase PTPMT1. PloS one 9, e93896 [PubMed: 24709986]
31. Niemi NM, Lanning NJ, Klomp JA, Tait SW, Xu Y, Dykema KJ, Murphy LO, Gaither LA, Xu HE, Furge KA, Green DR, and MacKeigan JP (2011) MK-STYX, a catalytically inactive phosphatase

regulating mitochondrially dependent apoptosis. Molecular and cellular biology 31, 1357–1368 [PubMed: 21262771]

32. Wishart MJ, and Dixon JE (2002) The archetype STYX/dead-phosphatase complexes with a spermatid mRNA-binding protein and is essential for normal sperm production. Proceedings of the National Academy of Sciences of the United States of America 99, 2112–2117 [PubMed: 11842224]
33. Banks DA, Dahal A, McFarland AG, Flowers BM, Stephens CA, Swack B, Gugssa A, Anderson WA, and Hinton SD (2017) MK-STYX Alters the Morphology of Primary Neurons, and Outgrowths in MK-STYX Overexpressing PC-12 Cells Develop a Neuronal Phenotype. Frontiers in molecular biosciences 4, 76 [PubMed: 29250526]
34. Dahal A, and Hinton SD (2017) Antagonistic roles for STYX pseudophosphatases in neurite outgrowth. Biochemical Society transactions 45, 381–387 [PubMed: 28408478]
35. Cao Y, Banks DA, Mattei AM, Riddick AT, Reed KM, Zhang AM, Pickering ES, and Hinton SD (2019) Pseudophosphatase MK-STYX Alters Histone Deacetylase 6 Cytoplasmic Localization, Decreases Its Phosphorylation, and Increases Detyrosination of Tubulin. International journal of molecular sciences 20
36. Qi Y, Kuang D, Kelley K, Buchser WJ, and Hinton SD (2022) Evolutionary genomic relationships and coupling in MK-STYX and STYX pseudophosphatases. Scientific reports 12, 4139 [PubMed: 35264672]
37. Thomas MG, Loschi M, Desbats MA, and Boccaccio GL (2010) RNA granules: The good, the bad and the ugly. Cell Signal
38. Anderson P, and Kedersha N (2006) RNA granules. J Cell Biol 172, 803–808 [PubMed: 16520386]
39. Sheehan CT, Hampton TH, and Madden DR (2022) Tryptophan mutations in G3BP1 tune the stability of a cellular signaling hub by weakening transient interactions with Caprin1 and USP10. The Journal of biological chemistry, 102552 [PubMed: 36183834]
40. Gallouzi IE, Parker F, Chebli K, Maurier F, Labourier E, Barlat I, Capony JP, Tocque B, and Tazi J (1998) A novel phosphorylation-dependent RNase activity of GAP-SH3 binding protein: a potential link between signal transduction and RNA stability. Mol Cell Biol 18, 3956–3965 [PubMed: 9632780]
41. Wehner KA, Schutz S, and Sarnow P (2010) OGFOD1, a novel modulator of eukaryotic translation initiation factor 2alpha phosphorylation and the cellular response to stress. Mol Cell Biol 30, 2006–2016 [PubMed: 20154146]
42. Tourriere H, Gallouzi IE, Chebli K, Capony JP, Mouaikel J, van der Geer P, and Tazi J (2001) RasGAP-associated endoribonuclease G3Bp: selective RNA degradation and phosphorylation-dependent localization. Mol Cell Biol 21, 7747–7760 [PubMed: 11604510]
43. Solomon S, Xu Y, Wang B, David MD, Schubert P, Kennedy D, and Schrader JW (2007) Distinct structural features of caprin-1 mediate its interaction with G3BP-1 and its induction of phosphorylation of eukaryotic translation initiation factor 2alpha, entry to cytoplasmic stress granules, and selective interaction with a subset of mRNAs. Mol Cell Biol 27, 2324–2342 [PubMed: 17210633]
44. Reiterer V, Fey D, Kolch W, Kholodenko BN, and Farhan H (2013) Pseudophosphatase STYX modulates cell-fate decisions and cell migration by spatiotemporal regulation of ERK1/2. Proceedings of the National Academy of Sciences of the United States of America 110, E2934–2943 [PubMed: 23847209]
45. Irvine K, Stirling R, Hume D, and Kennedy D (2004) Rasputin, more promiscuous than ever: a review of G3BP. The International journal of developmental biology 48, 1065–1077 [PubMed: 15602692]
46. Sahoo PK, Kar AN, Samra N, Terenzio M, Patel P, Lee SJ, Miller S, Thames E, Jones B, Kawaguchi R, Coppola G, Fainzilber M, and Twiss JL (2020) A Ca(2+)-Dependent Switch Activates Axonal Casein Kinase 2alpha Translation and Drives G3BP1 Granule Disassembly for Axon Regeneration. Current biology : CB 30, 4882–4895 e4886 [PubMed: 33065005]
47. Wolozin B, and Ivanov P (2019) Stress granules and neurodegeneration. Nature reviews. Neuroscience 20, 649–666 [PubMed: 31582840]

48. Advani VM, and Ivanov P (2020) Stress granule subtypes: an emerging link to neurodegeneration. Cellular and molecular life sciences : CMLS 77, 4827–4845 [PubMed: 32500266]

49. Allison LA (2021) Fundamentals of Molecular Biology. 110

50. Walkenhorst WF, Merzlyakov M, Hristova K, and Wimley WC (2009) Polar residues in transmembrane helices can decrease electrophoretic mobility in polyacrylamide gels without causing helix dimerization. Biochimica et biophysica acta 1788, 1321–1331 [PubMed: 19265670]

51. Rath A, Glibowicka M, Nadeau VG, Chen G, and Deber CM (2009) Detergent binding explains anomalous SDS-PAGE migration of membrane proteins. Proceedings of the National Academy of Sciences of the United States of America 106, 1760–1765 [PubMed: 19181854]

Highlights

- MK-STYX interacts with G3BP1 through its dual-specificity (DUSP) domain.
- The DUSP domain is required for MK-STYX-mediated decrease of stress granules.
- Tyrosine phosphorylation of G3BP1 is decreased in the presence of the DUSP domain.
- Stress granules appear morphological different with various domains of MK-STYX.

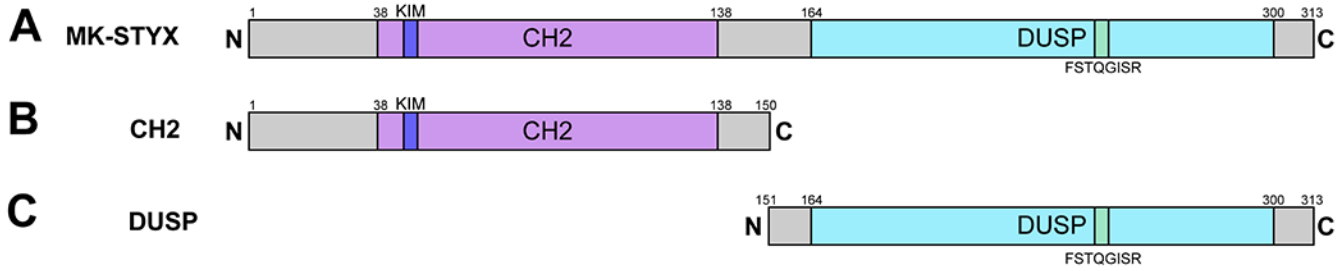

Figure 1. Schematic diagram of MK-STYX functional domains.

(A) Full length MK-STYX consists of the N-terminus CH2 domain with the kinase interacting motif (KIM) and the C-terminus DUSP domain signature active motif that exists as FSX_5R, instead of the HCX_5R required for catalysis. **(B)** The truncated CH2 domain from residues 1-150. **(C)** The truncated DUSP domain from residues 152-313.

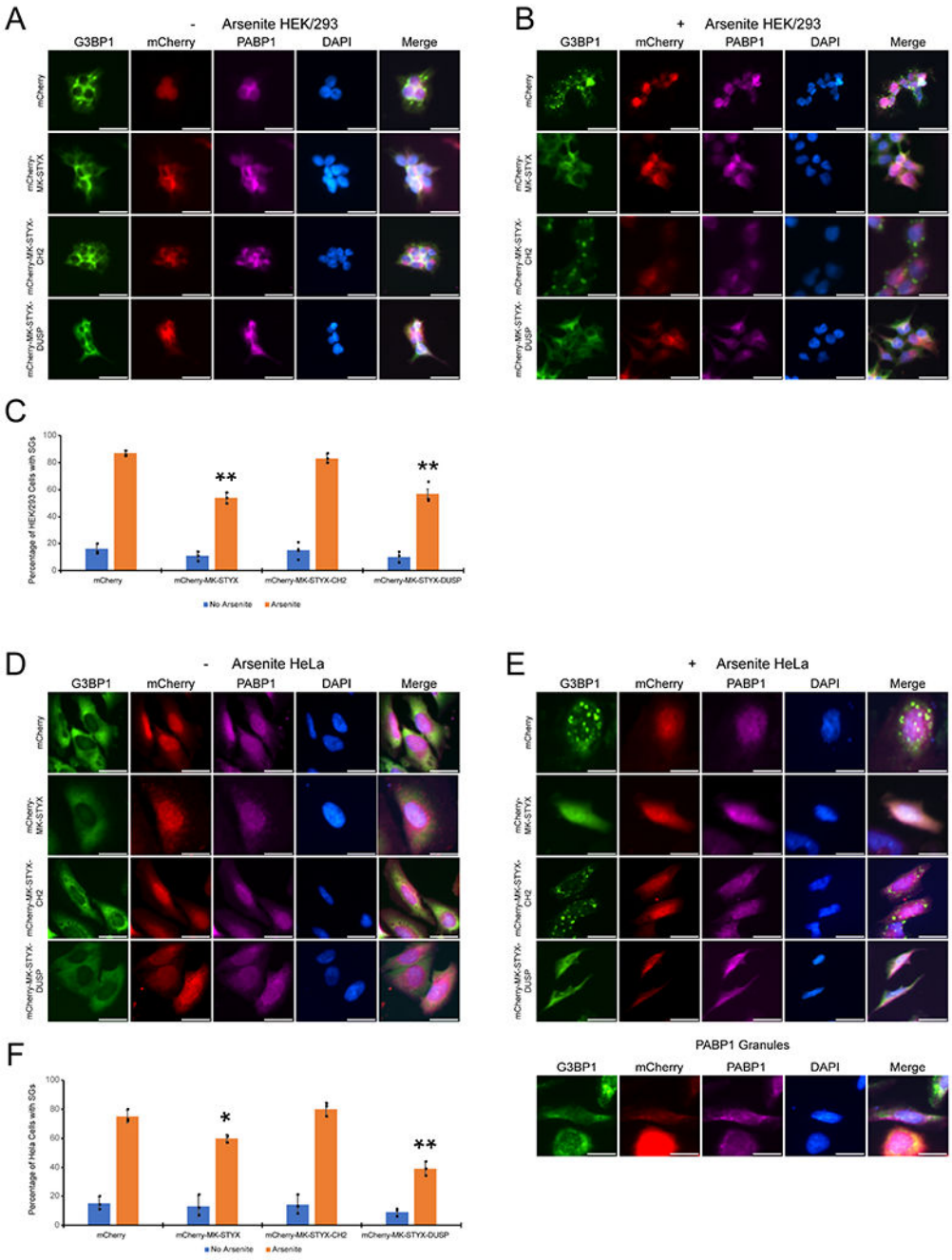

Figure 2. The DUSP Domain of MK-STYX inhibits arsenite-induced stress granule formation.

Representative examples are presented to illustrate the subcellular distribution of endogenous G3BP1 without arsenite treatment. **(A)** unstimulated HEK/293 cells or **(B)** following stimulation with 500 μM sodium arsenite in the absence (No Treatment) or presence of MK-STYX constructs. Cells were fixed, stained with anti-G3BP and FITC-conjugated goat anti-mouse antibodies, anti-PABP1-Cy5-conjugated antibodies and DAPI, and analyzed 24 h post-transfection for arsenite-induced stress granule formation by fluorescence microscopy. Merged images show the location of endogenous G3BP (green)

and PABP1 (purple) relative to the DAPI-stained nucleus (blue). **D)** HeLa cells or following stimulation with 500 μM sodium arsenite in the absence (No Treatment) or **(E)** presence of MK-STYX constructs. Cells were fixed, stained with anti-G3BP and FITC-conjugated goat anti-mouse antibodies, anti-PABP1-Cy5-conjugated antibodies and DAPI, and analyzed 24 h post-transfection for arsenite-induced stress granule formation by fluorescence microscopy. **(C and F)** Cells were scored for the presence and absence of stress granules. Bars represent the mean ± SEM. Asterisks indicate significant (*; p , 0.05 or ** p < 0.005) decrease compared to control cells (G3BP1-GFP and mCherry expressing cells), where ± 3.8 (HEK) or ± 4.6 (HeLA) standard deviation (SD) for G3BP1 and (mCherry); ± 3.5 SD (HEK) or ± 7.09 SD (HeLa) (mCherry-MK-STYX); ± 1.4 SD (HEK) or ± 6.6 SD (HeLa) (mCherry-MK-STYX-CH2) or ± 4.04 SD (HEK) or ± 2.6 SD (HeLa) (mCherry-MK-STYX-DUSP). ANOVA and Tukey's post-hoc also was used to calculate the statistically significant difference of each condition. Scale bar, 10 μm. (Three replicate experiments were performed (n = 100 cells for each experiment); the results are ± SD.

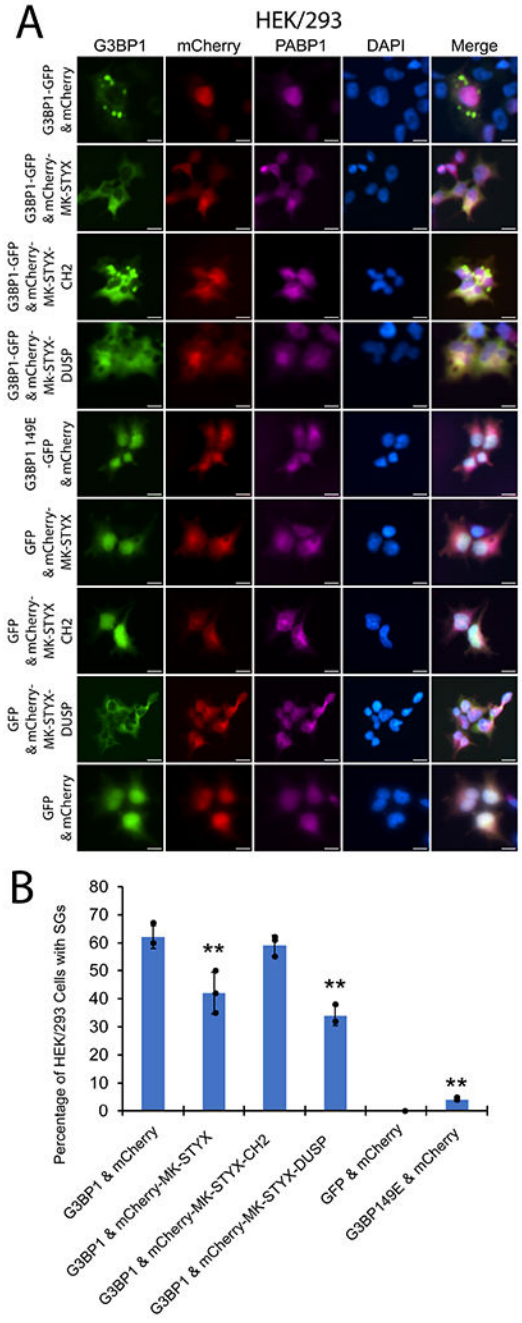

Figure 3. The DUSP domain of MK-STYX decreases G3BP1-induced stress granule formation.

(A) Representative examples of the subcellular distribution patterns of G3BP1. **(A)** HEK/293 cells co-transfected with expression vectors for G3BP1 and either wild-type or the DUSP domain of MK-STYX (mCherry-MK-STYX-DUSP) showed fewer cells with fully formed stress granules. The coexpression of G3BP1 and mCherry or G3BP1 and the CH2 domain of MK-STYX (mCherry-MK-STYX-CH2) resulted in mostly complete perinuclear stress granule formation. Cells co-transfected with G3BP1 and MK-STYX or the DUSP domain showed G3BP1 dispersed throughout the cells. Co-transfection with GFP and wild-

type MK-STYX, CH2 domain or DUSP domain showed no accumulation of granules. Co-transfection with G3BP1-S149E and mCherry also showed no accumulation. Merged images show the location of GFP-tagged G3BP1 (green) relative to mCherry-tagged MK-STYX or its domains (red) and the DAPI-stained nucleus (blue). Scale bar, 10 μm. **(B)** Quantitative analysis of HEK/293 cells represented in panel A. Data with cells co-expressing GFP and MK-STYX constructs formed no granules thus data was not plotted. Cells were analyzed 24 h post-transfection for G3BP1-induced stress granule formation, expression of MK-STYX constructs, and PABP1 by fluorescence microscopy, after staining with anti-PABP1-Cy5 and the DNA stain DAPI to reveal the nucleus. Cells were scored for the presence or absence of G3BP1 induced stress granules. Three replicate experiments were performed (n=100); the results are the ± SD Bars indicate the percentage of cells with stress granule formation. **$p<0.005$; n.s., $p>0.05$ decrease compared to control cells (G3BP1-GFP and mCherry expressing cells), where ± 3.2 standard deviation (SD) for G3BP1 and (mCherry); ± 6.1 SD (mCherry-MK-STYX); ± 3.1 SD (mCherry-MK-STYX-CH2) or 2.8 SD (mCherry-MK-STYX-DUSP); ± 0.5 SD for G3BP1-S149E and mCherry. ANOVA and Tukey's post-hoc also was used to calculate the statistically significant difference of each condition.

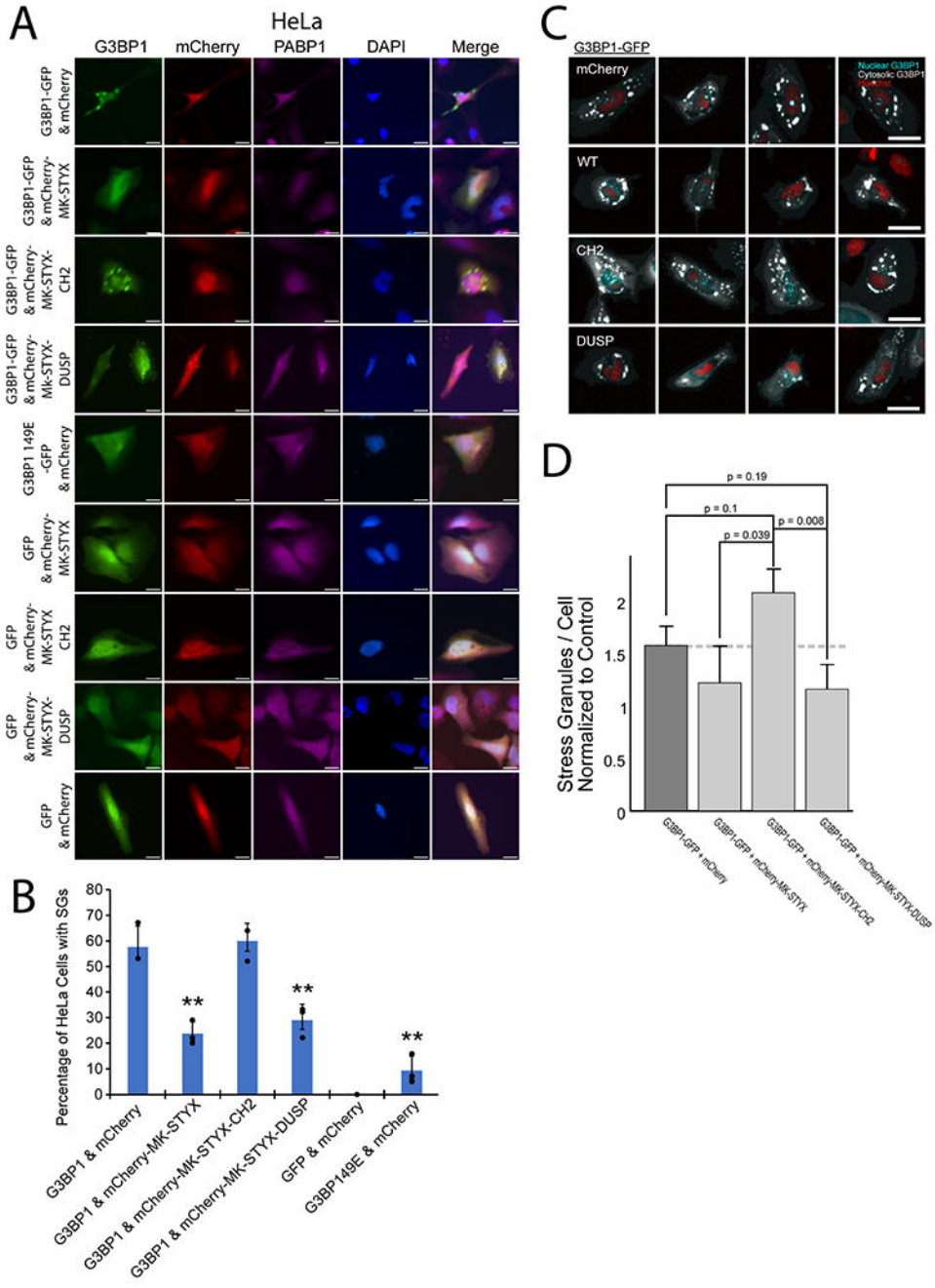

Figure 4. Representative examples of the subcellular distribution patterns of G3BP1.

(A) HeLa cells co-transfected with expression vectors for G3BP1 and either wild-type or the DUSP domain of MK-STYX (mCherry-MK-STYX-DUSP) showed fewer cells with fully formed stress granules. The coexpression of G3BP1 and mCherry or G3BP1 and the CH2 domain of MK-STYX (mCherry-MK-STYX-CH2) resulted in mostly complete perinuclear stress granule formation (arrow). Cells co-transfected with G3BP1 and MK-STYX or the DUSP domain showed G3BP1 dispersed throughout the cells. Co-transfection with GFP and wild-type MK-STYX, CH2 domain or DUSP domain showed no accumulation of

granules. Co-transfection with G3BP1-S149E and mCherry also showed no accumulation. Merged images show the location of GFP-tagged G3BP1 (green) relative to mCherry-tagged MK-STYX or its domains (red) and the DAPI-stained nucleus (blue). Scale bar, 10 μm. **(B)** Quantitated analysis of HeLa cells represented in panel A. Data with cells co-expressing GFP and MK-STYX constructs formed no granules thus data was not plotted. Cells were analyzed 24 h post-transfection for G3BP1-induced stress granule formation, expression of MK-STYX constructs, and PABP1 by fluorescence microscopy, after staining with anti-PABP1-Cy5 and the DNA stain DAPI to reveal the nucleus. Cells were scored for the presence or absence of G3BP1 induced stress granules. Three replicate experiments were performed (n=100); the results are the ± SD Bars indicate the percentage of cells with stress granule formation. **p<0.005; n.s., p>0.05. decrease compared to control cells (G3BP1-GFP and mCherry expressing cells), where ± 8.1 standard deviation (SD) for G3BP1 and (mCherry); ± 4.7 SD (mCherry-MK-STYX); ± 6.9 SD (mCherry-MK-STYX-CH2) or 6.1 SD (mCherry-MK-STYX-DUSP); ± 5.7 SD for G3BP1-S149E and mCherry. ANOVA and ad hoc Tukey was also used to calculate the statistically significant difference of each condition. **(C-D)** The CH2 domain of MK-STYX increases the number of stress granules per cell. **(C)** Representative examples of live HeLa cells showing the subcellular distribution patterns of G3BP1-GFP when co-transfected with mCherry, mCherry-MK-STYX, mCherry-MK-STYX-CH2 or mCherry-MK-STYX-DUSP. Only cells with stress granules were analyzed, which is appropriate to analyze the number of stress granule per cells. Stress granules cannot be counted in cells that do not express granules. **(C)** Merged images show the localization of GFP-tagged G3BP1 aggregates (white) as well as GFP-tagged G3BP1 dispersion within the nucleus (blue) in relation to the Hoechst-stained nucleus (red). Scale bar is 25 μm. **(D)** Bar chart showing the average number of G3BP1-induced stress granules normalized to control per cell, which is why the y-axis is at 2 and not the exact number stress granules per cell. Cells were plated with an automated liquid handler, grown for 24 hours, then stained and imaged with a confocal microscope and traced with the software InCarta. Eight replicate experiments were performed and cells (n=~250) were scored.

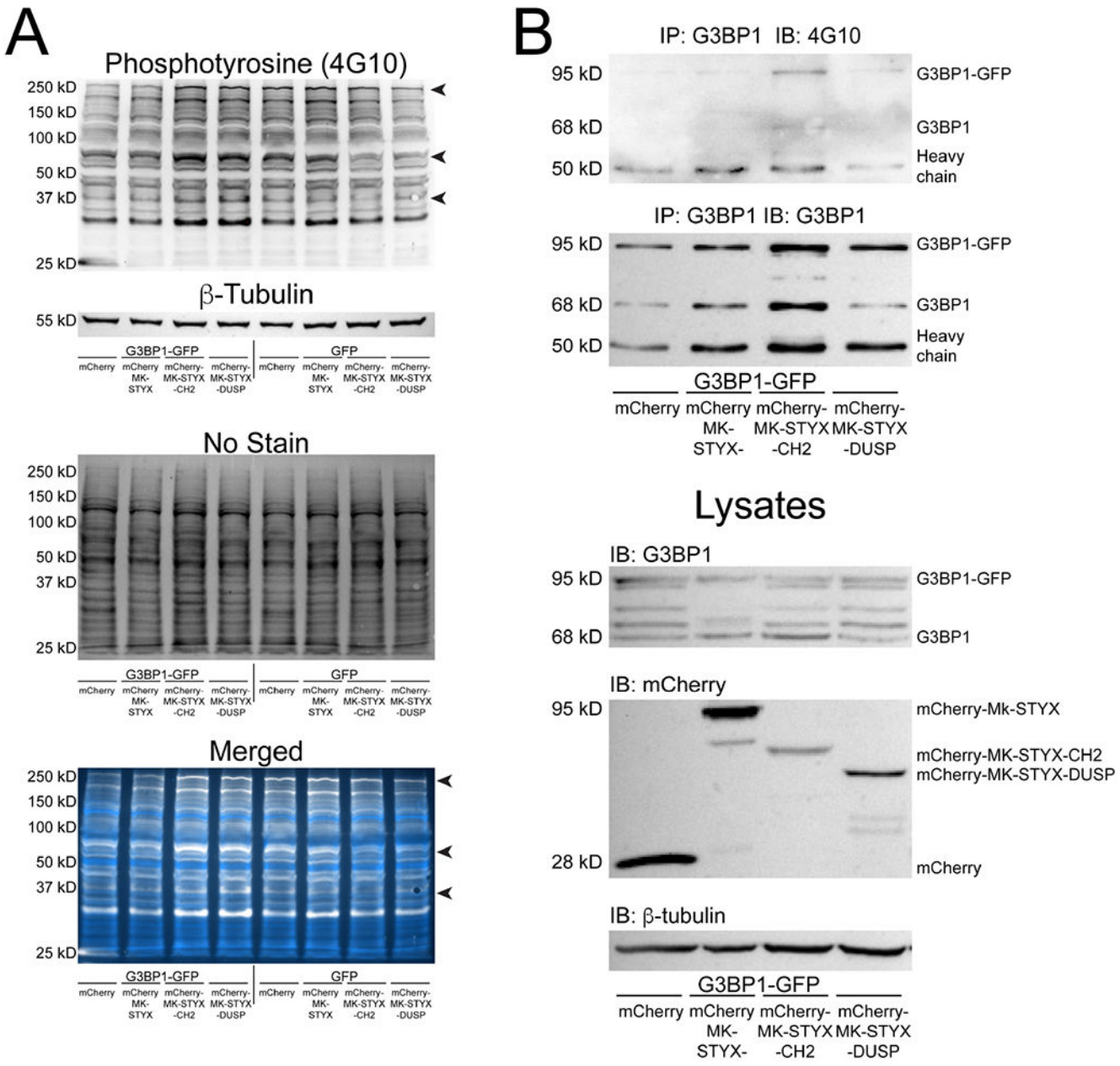

Figure 5. The DUSP domain of MK-STYX interacts with G3BP1.

HEK/293 cells co-transfected with expression vectors for G3BP1 of GFP and either mcherry (control), mCherry-tagged wild-type or the DUSP domain of MK-STYX (mCherry-MK-STYX-DUSP). **(A)** G3BP1 was immunoprecipitated (IP) from cell lysates with anti-G3BP1 antibodies or mCherry (middle panel) antibodies and in each case followed by immunoblotting (IB) with anti-mCherry or anti-G3BP1 (middle panel) antibodies to investigate the extent of binding. Wild-type MK-STYX and the DUSP domain co-immunoprecipitated with G3BP1 and in reciprocal studies endogenous G3BP1and G3BP1-GFP co-precipitated with the DUSP domain MK-STYX (mCherry-DSUP-MK-STYX). Similar results were obtained from multiple replicate experiments. **(B)** The

immunoprecipitation was validated by probing with anti-G3BP antibodies and anti-mCherry antibodies. **(C-F)** Lysates used to perform the IP experiments were analyzed with **(C)** anti-G3BP1 antibodies; **(D)** anti-GFP antibodies; **(E)** anti-mCherry antibodies; and **(F)** anti-β tubulin antibodies to detect the presence of protein and determine the equal loading of lysates. The expected kD for CH2 domain and DUSP domain is 46kD and 47 kD, respectively. DUSP resolved at the expected molecular weight; however, CH2 resolved at a higher molecular weight, above 50 kD. The CH2 domain consists of more residues that make up the “loop”, which separates the CH2 and DUSP domains (18) that may alter its charge and/or folding to interfere with its migration. It is common for proteins to resolve at higher expected weights due to net charge, post-translation modification, isoforms, etc. (50,51).

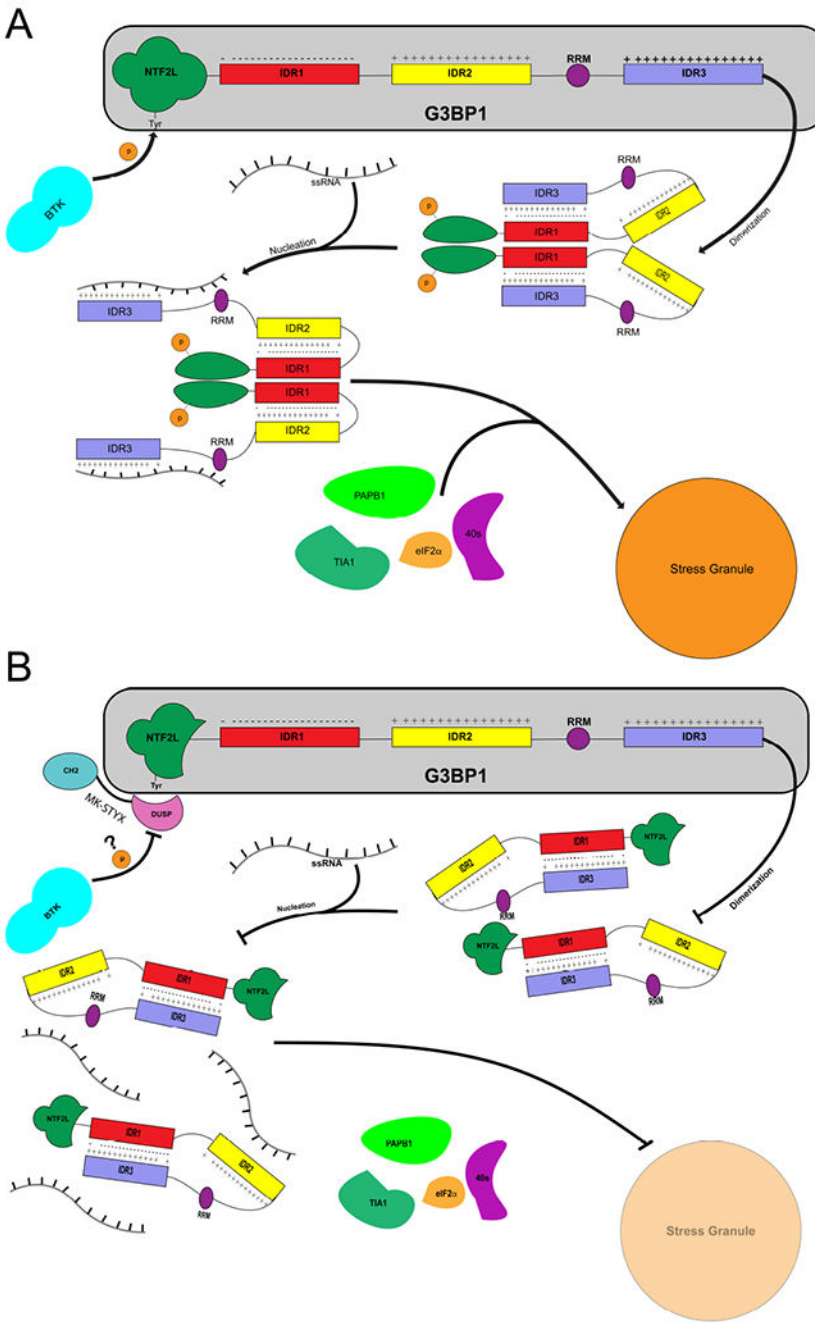

Figure 6. The DUSP domain of MK-STYX increases the phosphotyrosine phosphorylation of G3BP1.

HEK/293 cells co-transfected with expression vectors for G3BP1or GFP and either mcherry (control), mCherry-tagged wild-type or the DUSP domain of MK-STYX (mCherry-MK-STYX-DUSP) were lysed with buffer treated with phosphoprotein inhibitors and sodium orthovandate and analyzed by immunoblotting. Blots were probed with anti-phosphotyrosine, clone 4G10 antibodies and No-Stain for total protein lysate. **(A)** A change in tyrosine phosphorylation patten was observed such as proteins at ~ 75 Kd, 37 Kd, and

higher molecular weight, which are labeled with black arrows for ECL and Merged images. **(B)** G3BP1 was IP from cell lysates with anti-G3BP antibodies and in each case followed by IB with anti-G3BP1 antibodies to determine the tyrosine phosphorylation pattern of G3BP1. These anti-phosphotyrosine, clone 4G10 blots were performed on IPs used to determine interaction of G3BP1 and the domains of MK-STYX (Figure 4). Therefore, the blots with anti-G3BP1 antibodies for the IP and lysates were not re-probed and part of it were used for this figure. Tyrosine phosphorylation is required for G3BP1 induced stress granules (22). The phosphorylation of G3BP1 was increased in the presence of CH2 domain. Whereas the pG3BP1 was not in the presence of wild-type MK-STYX or the DUSP domain of MK-STYX.

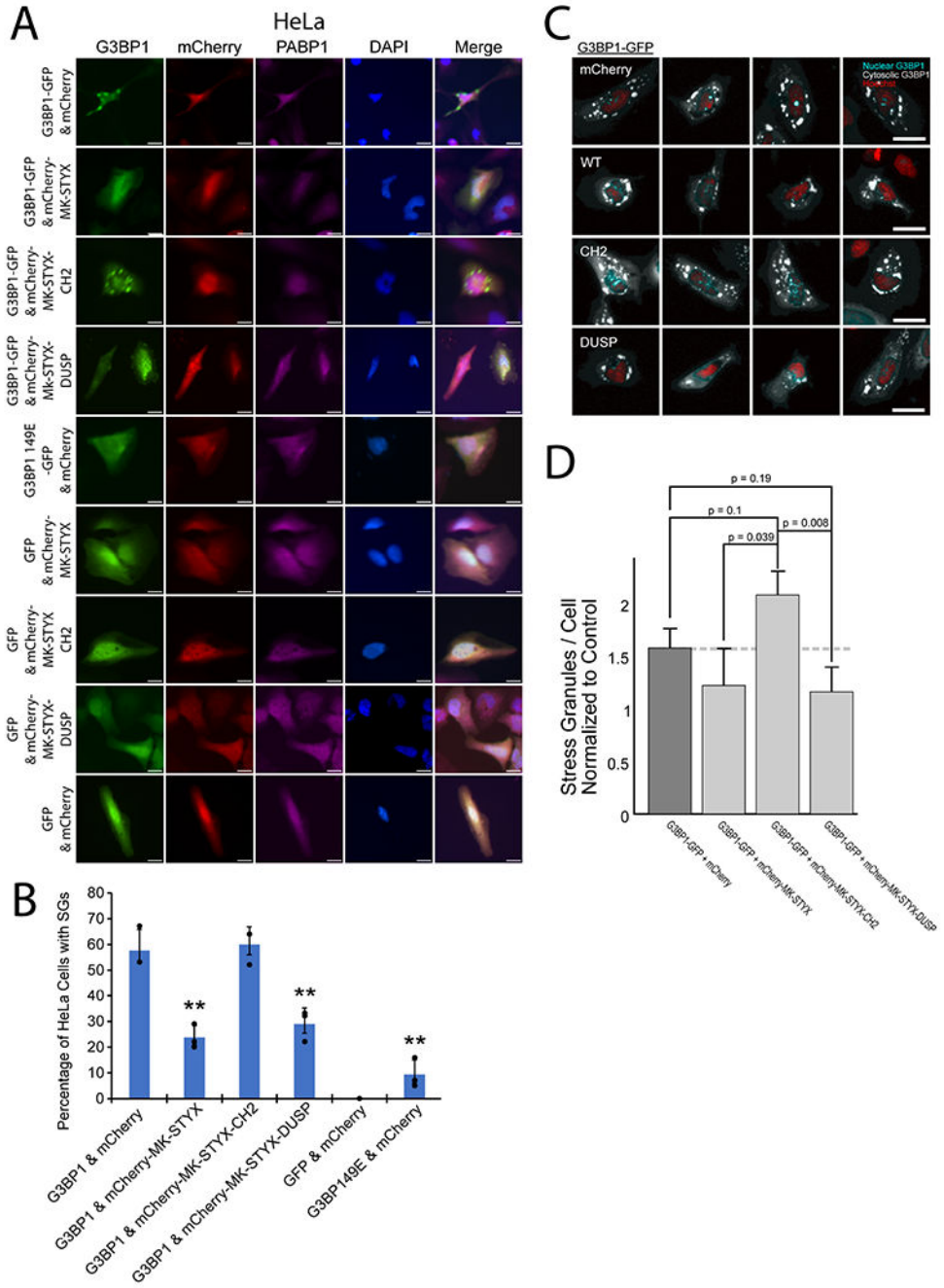

Figure 7: Speculative model of how MK-STYX decreases stress granules.

(A) BTK phosphorylates G3BP1 at tyrosine 40, enabling G3BP1 oligomerization. The dimer remains in a closed state due to the intramolecular interaction between the acidic IDR1 and basic IDR3, rendering it unable to bind single stranded (ssRNA). Increased ssRNA concentration within the cytosol displacing the interaction between ssRNA IDR1 and IDR3, preventing G3BP1 from serving as a seed for SG formation (nucleation). The G3BP1-ssRNA seed matures into a stress granule with the inclusion of additional RNA-binding proteins and ribosomal subunits such as PAPB1, T-cell intracellular antigen-1 (TIA-1),

eukaryotic initiation factor-2α. eIF2, etc. **(B)** MK-STYX through its DUSP domain masks the tyrosine 40 residue within the NTF2L domain of G3BP1, preventing phosphorylation by BTK. G3BP1 is unable to oligomerize and serve as a seed, impeding the formation of SGs. ssRNA. IDR1/3 is the intrinsically disordered region 1/3 of G3BP1.